Optimization of non-thermal plasma process to remove methyl blue towards application in wastewater treatment

Quoc-Phong Ho[1], Hoang-Nam Truong[1], Phuc-Thong Lam[1], Bich-Thuyen Nguyen Thi[1],
Van-Dung Nguyen[2], Pham Huu Ha-Giang[3], and Lien-Huong Huynh[1,*]

[1]*Faculty of Chemical Engineering, College of Engineering Technology, Can Tho University, Viet Nam*

[2]*Faculty of Electrical Engineering, College of Engineering Technology, Can Tho University, Viet Nam*

[3]*Faculty of Transportation Engineering, College of Engineering Technology, Can Tho University, Viet Nam*

*Corresponding author (hqphong@ctu.edu.vn)

Article info.

ABSTRACT

This study was carried out to optimize the treatment process of methyl blue (MB) in aqueous solution using dielectric barrier discharge (DBD) plasma and experiments were designed by using response surface methodology and central composite design (RSM-CCD). Four independent factors such as plasma power, liquid flow rate, air flow rate, and exposure time were investigated. According to the analyzed results of RSM, the experimental data is best fitted with a model of the quadratic polynomial with regression coefficient values of more than 0.9 for all responses. At optimal degradation conditions, the plasma power, liquid flow rate, air flow rate, and exposure time were 100 W, 1.5 lpm, 6 lpm, and 108.8 minutes respectively and the concentration of methyl blue was reduced to 95.8% with a concentration of 1.06 ppm. The degradation of methyl blue followed kinetic reaction rate was $r = 1.6 \times 10^{-3} [MB]^{2.2}$.

1. INTRODUCTION

During the past decade, dyeing and printing have been considered the major pollutants in total industrial sewage (De Moraes et al., 2000). These hazards are not only affecting the environment but also human health due to their complex composition, toxic and poor biodegradability (Capocelli et al., 2012). In addition, modern dyes are often manufactured to resist decomposition with long-term exposure to sunlight, water, and other harsh conditions. Therefore, finding the treatment method to decompose the dyeing wastewater faces many challenges. The treatment method often used is advanced oxidation processes (AOPs).

AOPs are chemical treatment procedures remove organic (and sometimes inorganic) compounds in water and wastewater based on oxidation the

reaction of hydroxyl radicals ($\cdot$OH) with the organic compounds (Glaze et al., 1987). Some of AOPs are considered such as electrochemical oxidation process (EOP's), Fenton/ Photo-fenton process, photocatalytic process, and electrical discharge plasma (Abedi et al., 2015; Wang et al., 2016).

Based on the temperature, the plasma method is classified into thermal plasma and non-thermal plasma (Bogaerts et al., 2002). Thermal plasma in which the temperature of electrons, ions, and gas is very high 2,000°C-20,000°C is usually produced at high pressure by direct current (DC), alternating current (AC), radio frequency (RF), and microwave source (Schriver et al., 1998). Non-thermal plasma is produced the same way, but the temperature of the ion and the gas is approximately the same as that of the environment. Non-thermal dielectric barrier

discharge plasma (DBD) is one of the most common types of non-thermal plasma, which is performed on a system of two parallel panel electrodes, or two coaxial poles separated by a thin insulating layer. Normally, the DBD device operates at a voltage of 10 - 20 kV with a frequency of 0.5-500kHz. The

DBD working at atmospheric pressure has been applied in water treatment, surface treatment, ozone generation, and sterilization in biomedical (Braithwaite, 2000; Bogaerts et al., 2002). The DBD plasma column or reactor is shown in the following Figure 1.
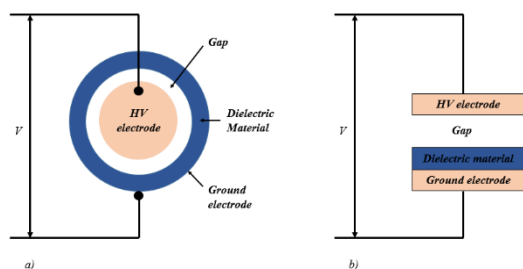

Figure 1. DBD plasma reactor arrangements according to the barrier discharge: a) cylindrical and b) planar

Non-thermal plasma is regarded as one of the high potential technologies of wastewater treatment and has been enormously studied for several decades. According to recent studies, they reported that the use of atmospheric non-thermal plasma for the degradation of several organic pollutants in aqueous water like methyl orange (MO) and rhodamine-B (RB) were completely removed at concentrations roughly 10^{-4} M (Bansode et al., 2017). Methyl blue (MB) is usually used as a stain in histology, printing and colouring.

Treatment of MB in aqueous solution was influenced by multiple variables during previous laboratory experiments (unpublished data) which are shown in Table 1. According to these previous experimental data, the central point for each independent variable is determined, and the appropriate experimental setup for the optimization process is then constructed. Therefore, optimization in degradation of MB is to investigate the relationship between independent variables and response variables. In this study, the response surface methodology (RSM) was applied to optimize the degradation process (Li et al., 2017). The objective of the study aims to obtain the lowest final concentration of MB and highest degradation percentage.

Table 1. Screening study for optimization of MB degradation

Independent variable	Range of factor	Optimal value
Power (W)	40 → 120	100
Liquid flowrate (lpm)	1 → 5	2
Air flowrate (lpm)	2 → 8	5
Exposure time (min)	30 → 240	120
Initial concentration (ppm)	10 → 100	25

2. MATERIALS AND METHOD

2.1. Materials

Methyl blue (Acid blue 93, $C_{37}H_{27}N_3Na_2O_9S_3$, 799.80 g.mol^{-1}, λ_{max} = 663 nm) was obtained from Sigma-Aldrich USA, purified water produced by Biotechnology Research & Development Institute, Can Tho University.

2.2. DBD plasma system and operation

This study used the non-thermal DBD plasma system with coaxial electrode (Figure 2). The coaxial electrode consisted of the inner electrode made of stainless steel (22 mm in diameter) (1) and the outer electrode made of aluminum foil (0.08 mm in diameter). An insulating barrier was made by a quartz tube whose inner and outer diameters were 29 mm and 35 mm, respectively. Cold plasma was created between the water layer of the electrode and the inner surface of the quartz tube due to the appearance of micro-discharges. Air was supplied into the plasma chamber to enhance ozone in the water solution using an electric pump (4). The ozone was formed at the outside plasma chamber because of the interaction between corona discharges and oxygen in the air. The generated ozone was transferred to the bottom of the storage tank to increase the efficiency of ozone dissolution in water.

The system was operated as follows: 8 liters of MB solution was prepared in container (3), opened the valve removing 4 liters of solution to the main container (2), and then closed the valve. The pumps were turned on, where pump (4) was for circulating solution and pump (5) was for providing oxygen for the indirect chamber. Samples will be drawn at a certain time and then stored at 5°C before being analyzed UV-Vis.
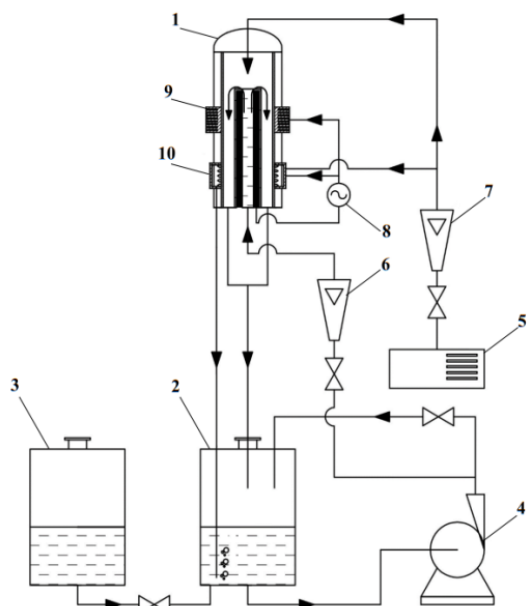
Figure 2. Non-thermal DBD plasma system: (1) plasma column, main solution container (2), auxiliary solution container (3), pump for solution flow (4), pump for airflow (5), liquid flowmeter (6), air flowmeter (7), high-voltage transformer (8), direct plasma chamber (9), and indirect plasma chamber (10)

2.3. Experimental design

The effect of independent variables such as power (X_1), liquid flow rate (X_2), air flow rate (X_3), exposure time (X_4) were investigated using response surface methodology (RSM). Response variables are MB final concentration (Y_1) and degradation percentage (Y_2). The experimental design based on the RSM-CCD is presented in Table 2.

Table 2. Experimental design using RSM-CCD

Independent variable	Symbol	Coded levels				
		$-\alpha$	-1	0	$+1$	$+\alpha$
Power, W	X_1	40	60	80	100	120
Liquid flow rate, lpm	X_2	1	1.5	2	2.5	3
Air flow rate, lpm	X_3	2	3	5	6	8
Exposure time, min	X_4	30	60	90	120	150

A second order polynomial equation was used to determine the predicted responses (degradation percentage) as a function of an independent variable as follows in equation (1):

$$Y\% = \beta_0 + \sum \beta_i X_i + \sum \beta_{ii} X_i^2 + \sum \sum \beta_{ij} X_i X_j \qquad (1)$$

where Xi is the coded value of the main factor; Y% is the response function; β0, βi, and βii are the constant, the first-order coefficient, and the squared coefficient of factor i, respectively; and βij coefficient is the interaction between factors i and j (Amiri & Sabour, 2014).

2.4. Analytical method

The MB solution after treatment will be measured pH and temperature immediately and concentration of MB solution was analyzed by UV-visible spectrophotometer (Perkin Elmer) at wavelength 663 nm according to the standard *TCVN 4581:1988*. The degradation percentage was determined by the following equation.

$$\text{Degradation percentage} \% = \frac{c_0 - c}{c_0} \times 100\% \quad (2)$$

Where C_o is initial concentration and C is concentration after treatment, respectively.

2.5. Statistical analysis

The best-fitting polynomial model was predicted by statistical parameters such as R-squared, adjusted R-squared, multiple correlation coefficients, and coefficients using Design Expert Software version 13. ANOVA analysis including analysis of variance, fit statistics, model comparison statistics, coded equations, and actual equations was used to assess whether the model was significant or nonsignificant, and the significance was based on calculating the F-value at probabilities of 0.01, 0.1, and 0.5.

3. RESULTS AND DISCUSSION

3.1. Fitting and the model

The coefficients of the polynomial equation calculated from experimental data based on the Design Expert Software used to make predictions of the response.

Table 3. Variables and response values

Run	Independent variables				Response values	
	X_1	X_2	X_3	X_4	Y_1(ppm)	Y_2(%)
1	120	2	4.5	90	2.24	91.04
2	100	1.5	6	120	1.05	95.78
3	80	2	4.5	30	6.64	73.45
4	80	2	4.5	90	4.98	80.07
5	100	2.5	3	120	3.56	85.75
6	80	1	4.5	90	6.50	73.98
7	100	2.5	3	60	4.21	83.15
8	80	2	4.5	90	4.95	80.19
9	100	1.5	6	60	3.53	85.89
10	60	1.5	6	60	7.75	69.00
11	60	2.5	6	120	7.75	69.00
12	60	2.5	3	120	6.42	74.30
13	80	2	7.5	90	3.39	86.45
14	100	1.5	3	60	4.19	83.24
15	80	2	4.5	90	4.74	81.05
16	60	1.5	6	120	6.75	73.00
17	80	2	4.5	90	4.64	81.45
18	60	1.5	3	60	10.50	58.00
19	60	1.5	3	120	10.00	60.00
20	80	2	4.5	90	4.69	81.25
21	80	3	4.5	90	5.06	79.76
22	40	2	4.5	90	13.69	45.25
23	80	2	1.5	90	6.03	75.90
24	60	2.5	3	60	8.13	67.50
25	100	2.5	6	60	4.11	83.56
26	100	1.5	3	120	2.75	89.00
27	80	2	4.5	150	1.71	93.15
28	60	2.5	6	60	9.25	63.00
29	80	2	4.5	90	4.75	81.00
30	100	2.5	6	120	1.64	93.45

Regression equations of each response variable including final concentration and degradation percentage achieved from RSM are listed in equations (3) and (4).

$$Y_1 = +43.44 - 0.49X_1 - 10.18X_2 - 1.26X_3$$
$$+0.05X_4 + 0.002X_1^2 + 1.04X_2^2 - 0.004X_3^2$$
$$-0.0002X_4^2 + 0.03X_1X_2 - 0.002X_1X_3$$
$$-0.0002X_1X_4 + 0.73X_2X_3 - 0.004X_2X_4$$
$$-0.004X_3X_4 \qquad (3)$$
$$Y_2 = -73.76 + 1.98X_1 + 40.73X_2 + 5.03X_3$$
$$-0.18X_4 - 0.008X_1^2 - 4.15X_2^2 + 0.02X_3^2$$
$$+0.0006X_4^2 - 0.14X_1X_2 + 0.007X_1X_3$$
$$+0.001X_1X_4 - 2.93X_2X_3 + 0.02X_2X_4$$
$$+0.02X_3X_4 \qquad (4)$$

The experimental results would be successfully performed with a quadratic polynomial model, with the coefficient of determination (R^2) value for both final concentration (Y_1) and degradation percentage

(Y_2) being 0.9686, according to the statistical analysis (ANOVA) stated in Table 4.

Table 4. Regression coefficients values

Regression coefficients	Y_1 (ppm)	Y_2 (%)
Intercept ($\alpha 0$)	4.79	80.84
X_1-Power ($\alpha 1$)	– 2.68	10.73
X_2-Liquid flow rate ($\alpha 2$)	– 0.18	0.7231
X_3-Air flow rate ($\alpha 3$)	– 0.55	2.20
X_4-Exposure time ($\alpha 4$)	– 0.89	3.60
X_1^2 ($\alpha 11$)	0.80	– 3.22
X_2^2 ($\alpha 22$)	0.26	– 1.04
X_3^2 ($\alpha 33$)	– 0.01	0.0399
X_4^2 ($\alpha 44$)	– 0.14	0.5711
X_1X_2 ($\alpha 12$)	0.34	– 1.36
X_1X_3 ($\alpha 13$)	– 0.05	0.2087
X_1X_4 ($\alpha 14$)	– 0.15	0.5834
X_2X_3 ($\alpha 23$)	0.55	– 2.19
X_2X_4 ($\alpha 24$)	– 0.06	0.2279
X_3X_4 ($\alpha 34$)	– 0.2	0.7888
R^2	0.9686	0.9686
Adjusted R^2	0.9393	0.9393
Model's F-value	33.05	33.05
Model's P-value	< 0.0001	< 0.0001

The results presented in Table 4 showed that the P-value of the model is smaller than 0.05 (P < 0.0001) for all variables, indicating that our model is statistically accurate. The model better fits the experimental data if the values of R^2 are closer to one and vice versa (Myers et al., 2016). The value of R^2 of both models is 0.9686 which is closer to one, indicating a strong relation between experimental data and predicted values (Figure 3), which means the responses are well-predicted. In addition, the value of adjusted R^2 reflects the influence of independent variables and these values for both models are 0.9393 indicating the more fitting between estimated and experimental values.

The influence of power (X_1), liquid flow rate (X_2), air flow rate (X_3), and exposure time (X_4) on response variables could be satisfactorily explained in this study using the quadratic polynomial model, as demonstrated by proximity to unity R^2. The significance of regression coefficients of the quadratic polynomial model was assessed by analysis of variance (ANOVA) in which a smaller P-value and a larger F-value indicate a highly significant influence on the response variables (Quanhong & Caili, 2005). In this study, the F-value and P-value are 33.05 and 0.0001, respectively which implies the model is significant.
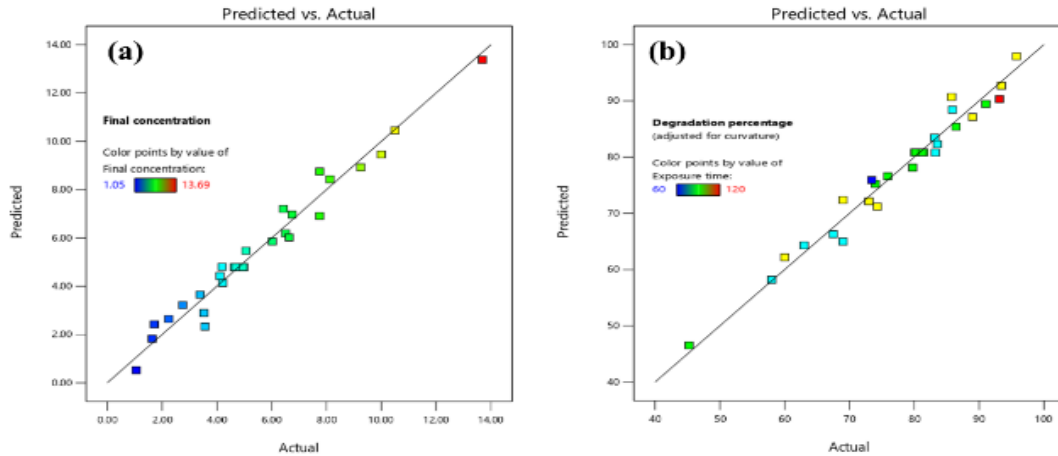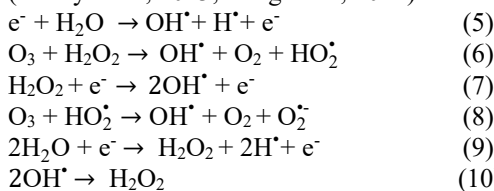
Figure 3. Relationship between actual and predicted responses for (a) final concentration, (b) degradation percentage.

3.2. Effect of the independent variables on response variables

MB was successfully treated utilizing a non-thermal DBD plasma process with many independent factors. Table 3 shows the influence of independent variables (power, liquid flow rate, air flow rate, and exposure time) on responses (remaining concentration and degradation percentage). Table 4 summarizes the regression coefficients for independent variables and their statistical meaning. The coefficients X_1, X_2, X_3, X_4, X_1^2, etc., represent the relationship between a predictor variable and the responses. The overall average response of all the runs is the intercept of the orthogonal design. The coefficients are adjustments around the average based on the factor settings. If the influence coefficient of a factor is positive, it means that the factor affects more at a high level, and conversely, if the influence value is a negative number, then that factor affects more at low a level with surveyed results.

Under the effect of plasma discharge, the formation of ozone and other components with strong oxidizing properties such as $^\bullet OH$, H_2O_2 was observed, etc., (Kogelschatz, 2003). The formation of the free radical mechanism during DBD plasma discharge will be elaborated in equations (5)-(10) (Reddy et al., 2013; Jiang et al., 2014)

$$e^- + H_2O \rightarrow OH^\bullet + H^\bullet + e^- \qquad (5)$$
$$O_3 + H_2O_2 \rightarrow OH^\bullet + O_2 + HO_2^\bullet \qquad (6)$$
$$H_2O_2 + e^- \rightarrow 2OH^\bullet + e^- \qquad (7)$$
$$O_3 + HO_2^\bullet \rightarrow OH^\bullet + O_2 + O_2^{\bullet -} \qquad (8)$$
$$2H_2O + e^- \rightarrow H_2O_2 + 2H^\bullet + e^- \qquad (9)$$
$$2OH^\bullet \rightarrow H_2O_2 \qquad (10)$$

$^\bullet OH$ radicals play a significant role in the DBD plasma treatment because of their high oxidation potential (Hemmert et al., 2003). The $^\bullet OH$ concentration, however, is difficult to detect due to its short lifespan (3.7×10^{-9} s) (Xiang et al., 2011). However, under plasma treatment, H_2O_2 an oxidation agent is also formed by the interaction between free electron and H_2O (Eq. 9) and the recombination of two $^\bullet OH$ radicals (Eq. 10) (Wang et al., 2016). The concentration of H_2O_2 generated can be considered an indirect tool for determining the $^\bullet OH$ in the plasma treatment process (Locke et al., 2006). As a result, plasma treatment is influenced by the amount of produced active species. Hence, the factors that influence the concentration of active species and the extent of their influence on the degradation of MB dye have been investigated to select the optimal process parameters. Power, liquid flow rate, air flow rate, and exposure time are all factors that should be considered. To optimize the treatment, it is required to investigate the extent of their effect and determine the most appropriate settings.

Response surface figures were created using design expert software to demonstrate the effects of power, liquid flow rate, air flow rate, and exposure time on response variables. These figures were constructed by altering two independent variables within experimental ranges while keeping the third variable constant. The three-dimensional response surfaces are used to analyze the models and experimental data, as well as to comprehend the interaction and primary impacts of independent variables. In Figure 4a-f, the influence of power (W), liquid flow rate

(lpm), air flow rate (lpm), and exposure time (min) on degradation percentage are illustrated, all these variables exert a linear effect on degradation percentage.

Different powers of plasma treatment were used in this study and based on the responses of models it found that an increase in power from 40 W to 120 W led to an increasing percentage of MB degradation. According to theoretical background, power (or plasma generating capacity) is a major factor influencing the generation of active species to participate in the main reaction of the process. The greater the power, the greater the plasma-generating energy, this energy helps to convert neutral molecules into ions, electrons, and free radicals. In addition to the interaction between plasma and chemical compounds, free radicals possess a very strong oxidizing ability, which helps in effectively decomposing organic compounds (Wardenier, 2016). Therefore, in this experiment, when increasing the plasma irradiation power, the degradation efficiency increases due to the impact of the plasma on the active substance, the plasma layer is generated quite thick, the higher energy makes the decomposition better. Moreover, in previous studies, scientists found that the formation of ozone, UV rays, and strong oxidizing agents, typically free hydroxyl $OH^{\bullet}$. Free radicals have strong oxidizing properties, O_3, and UV rays are generated, which effectively decompose organic and inorganic substances and bacteria. O_3, $OH^{\bullet}$ and UV rays are generated proportional to the machine power. Therefore, when increasing the capacity, the degradation percentage of MB also increases (Kuraica et al., 2006; Bai et al., 2010).
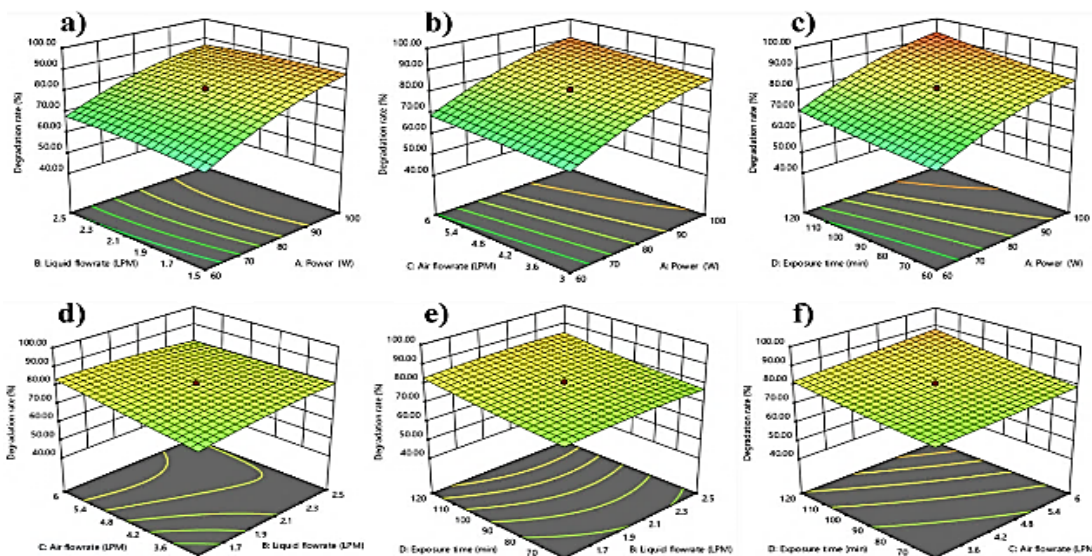

Figure 4. Response surfaces illustrating the influence of each parameter on degradation percentage levels

Degradation of MB is also affected by liquid flow rate and air flow rate. According to the results, an increase in both liquid flow rate and air flow rate had an ascending and descending trend on MB degradation percentage. The increased liquid flow rate increases the contact of the solution with the plasma layer, increasing the number of repetitions in the degradation process. Hence, when increasing the liquid flow rate, the ability to remove MB also increases, however, the treatment efficiency will decrease if the liquid flow rate is increased excessively. When the liquid flow rate is increased, the plasma energy generated will be evenly distributed to the part of the solution flowing through, and the interaction energy received by each molecule will decrease, because the plasma and the solution interact with each other within a certain period (Wardenier, 2016). Therefore, the interaction between oxidizing agents and free radicals with MB is also reduced, so the degradation ability is also reduced (Bai et al., 2010).

Moreover, in the plasma treatment, air plays a role in providing oxygen through the plasma layer to create free radicals and strong oxidizing agents such as $OH^{\bullet}$, $H^{\bullet}$, H_2O_2 and O_3. The free radicals and strong oxidizing agents above contribute

significantly to the decomposition of organic substances in water in general and MB in particular (Bai et al., 2010; Wardenier, 2016). According to the results, the air flow rate shows a similar trend to that of the liquid flow rate during plasma treatment. When the air flow rate is increased, the MB degradation percentage also increases, but when the air flow rate is far too large, the degradation percentage decreases. This is explained by the fact that elevating air flow rate too high increases the energy required for gas molecules, causing the portion of the energy interacting with MB to fluctuate.

One more important factor that should be taken into consideration is the exposure time in the plasma treatment. The results indicated that the longer the exposure time, the higher the MB degradation percentage. This explains that, when increasing the exposure time, the degradation percentage also increases due to the long-term contact between MB and the generated plasma. The amount of air passing through the plasma column and other remaining parameters as power and liquid flowrate are also stable over time. Furthermore, as the concentration of free radicals and oxidizing agents such as $OH^\bullet$, $H^\bullet$, H_2O_2 and O_3 in the solution increased over time, so did the degradation ability.

3.3. Optimization of independent variables

The desirability function was used to perform numerical optimization in Design Expert Software. The objectives were chosen for optimizing MB degradation with the appropriate operational parameters to achieve the minimum final concentration and the highest degradation percentage over 90%. The optimized MB degradation was chosen as the solution with the highest desirability value.

Table 5. Optimum conditions

Optimum Conditions	Coded Levels	Actual Levels
Power, W	1	100
Liquid flowrate, lpm	-1	1.5
Air flowrate, lpm	1	6
Exposure time, min	0.6	108.8

Combined optimized operational conditions for MB degradation were investigated at 100 W of generated plasma capacity, 1.5 lpm and 6 lpm for liquid flow rate and air flow rate, respectively, exposed in 108.8 minutes (Table 5). The response values at optimized degradation conditions were 1.055 ppm MB final concentration and reached 95.78% of the degradation percentage, illustrated in Table 5 and Figure 5.
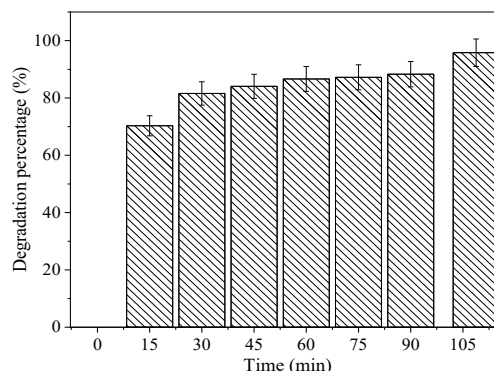

Figure 5. Degradation of MB at optimal conditions: power 100 W, liquid flowrate 1.5 lpm, air flowrate 6 lpm, exposure time 108.8 min

3.4. Verification of RSM model

The model's usefulness for predicting response values was tested under optimized MB degradation conditions. Experiments under optimized conditions were used to validate the optimized degradation conditions. At optimal degradation conditions, the response values were 1.055 ppm MB final concentration and a degradation percentage of 95.78 percent. The experimental values at optimal degradation circumstances, on the other hand, were 1.061 ppm MB final concentration and a degradation percentage of 95.75%. The experimental and expected reaction levels were quite similar in Table 5.

3.5. Effect of pH and temperature during plasma discharge

During the treatment, pH and temperature were measured to investigate the change. In general, pH tends to decrease gradually with treatment time. The difference in pH is clearly shown through the difference in power, when increasing the power, the treatment efficiency increases, and the pH decreases over time. The gradual decrease of pH can be explained that in the decomposition process, the acid compound, HNO_3 is formed during plasma interaction with methyl blue, hence the pH also decreases with time (Reddy et al., 2013). The change of pH is shown in Figure 6a.

Furthermore, the temperature of the sample is proportional to the increase in power and exposure time. The reason for this phenomenon is due to the resistance in the system as well as the friction of the sample against the wall of the reactor. In addition,

the increase in power also leads to electrical energy turning into heat, which leads to a gradual increase in temperature over time. The change in temperature is shown in Figure 6b.
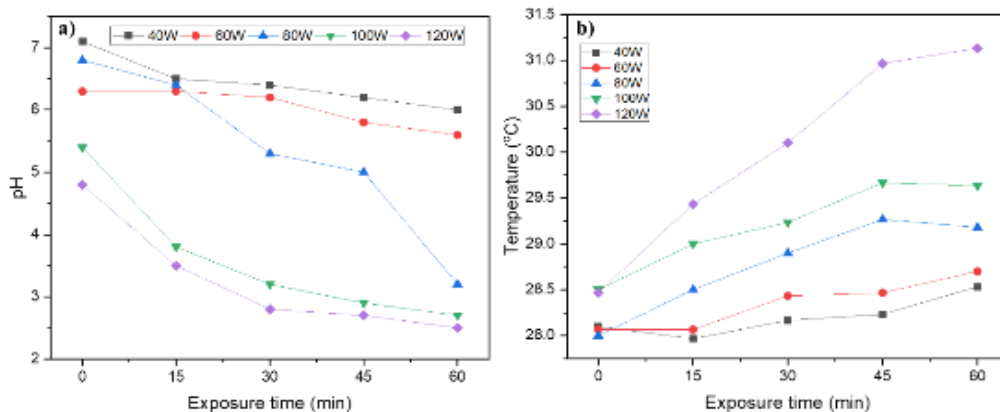

Figure 6. The change of pH (a), and temperature (b) in MB aqueous solution in different power in 60 minutes

3.6. Kinetics study

In this section, the data collected from the optimal experiment was applied to determine the reaction order based on the half-life method.

$$log\tau_{1/2} = log\frac{2^{n-1} - 1}{(n-1)k} - (n-1)log[MB]_0$$

The calculation of reaction order following the half-life method is illustrated in Table 6. The plots of $log\tau_{1/2}$ versus $log[MB]_0$ is shown in Figure 7, this logarithmic plot gives a straight line. The fitted line shows a correlation constant (R^2) of 0.99. The slope of this plot is -1.2. Hence, the reaction order is calculated by $1 - (-1.2) = 2.2$. The reaction is fitted second-order model. We also have:

$$log\frac{2^{n-1} - 1}{(n-1)k} = 2.8271 \rightarrow k = 1.6.10^{-3} ppm^{1.2}.min^{-1}$$

So, degradation rate of MB under plasma treatment:
$$r = 1.6.10^{-3} ppm^{-1.2}.min^{-1}[MB]^{2.2}$$

Table 6. Result of calculations for determination of reaction order by half-life method

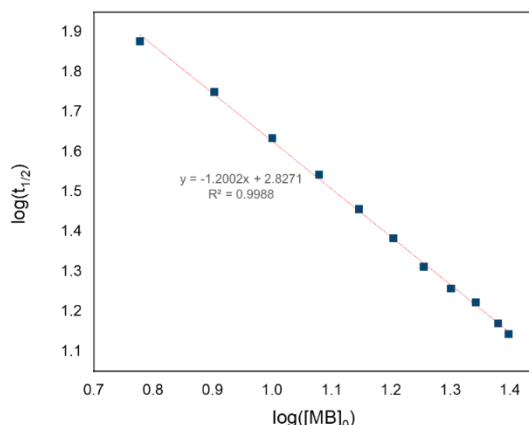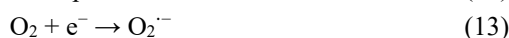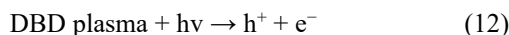| $[MB]_0 \rightarrow$ $[MB]$ (ppm)	$\tau_{1/2}$ (min)	Log($[MB]_0$)	Log($\tau_{1/2}$)
$25 \rightarrow 12.5$	13.9	1.40	1.14
$24 \rightarrow 12$	14.8	1.38	1.17
$22 \rightarrow 11$	16.7	1.34	1.22
$20 \rightarrow 10$	18.1	1.30	1.26
$18 \rightarrow 9$	20.5	1.26	1.31
$16 \rightarrow 8$	24.2	1.20	1.38
$14 \rightarrow 7$	28.6	1.15	1.46
$12 \rightarrow 6$	34.9	1.08	1.54
$10 \rightarrow 5$	43.1	1.00	1.63
$8 \rightarrow 4$	56.2	0.90	1.75
$6 \rightarrow 3$	75.4	0.78	1.88

Figure 7. Plots $log\tau_{1/2}$ versus $log[MB]_0$ for determination of reaction order

3.7. Mechanism for MB degradation

The degradation of color compounds under plasma irradiation is generally based on the bond-dissociation energy (BDE). The lower the BDE, the easier it is to break old bonds and form new ones (Huang et al., 2012). These oxy radicals, as well as other free radicals, can attack MB dye and cause it to degrade into degradation products (Li et al., 2011; Qutub et al., 2016).

The following is a proposed mechanism for dye degradation utilizing non-thermal plasma.

DBD plasma + hv → h⁺ + e⁻   (12)

O₂ + e⁻ → O₂·⁻   (13)

h⁺ + H₂O → H⁺ + OH·   (14)

$$O2^{\cdot -} + e^- + 2H^+ \rightarrow H_2O_2 \qquad (15)$$

$$H_2O_2 + e^- \rightarrow OH^- + OH^{\cdot} \qquad (16)$$

$$OH^{\cdot} + MB \rightarrow \text{Degradation products} \qquad (17)$$

4. CONCLUSION

The degradation conditions of methyl blue such as plasma power, liquid flow rate, air flow rate, and exposure time were investigated successfully. According to ANOVA analysis, the quadratic model was adequate for describing and predicting the reactions of MB final concentration and degradation percentage to changes in the independent variables.

The optimum condition was found using the desired function and numerical optimization. At optimal degradation conditions, the plasma power, liquid flowrate, air flowrate, and exposure time were 100W, 1.5 lpm, 6 lpm, and 108.8 minutes, respectively and the concentration of methyl blue (MB) was reduced to 95.8% with the concentration of 1.06 ppm. The study also found that the degradation of methyl blue followed by kinetic reaction rate was $r = 1.6.10^{-3}[MB]^{2.2}$. Furthermore, the effective treatment of MB provides potential for cold plasma application in wastewater treatment.

REFERENCES

Abedi, K., Ghorbani-Shahna, F., Jaleh, B., Bahrami, A., Yarahmadi, R., Haddadi, R., & Gandomi, M. (2015). Decomposition of chlorinated volatile organic compounds (CVOCs) using NTP coupled with TiO₂/GAC, ZnO/GAC, and TiO₂–ZnO/GAC in a plasma-assisted catalysis system. *Journal of Electrostatics*, *73*, 80-88.

Amiri, A., & Sabour, M. R. (2014). Multi-response optimization of Fenton process for applicability assessment in landfill leachate treatment. *Waste Management*, *34*(12), 2528-2536.

Bai, Y., Chen, J., Yang, Y., Guo, L., & Zhang, C. (2010). Degradation of organophosphorus pesticide induced by oxygen plasma: effects of operating parameters and reaction mechanisms. *Chemosphere*, *81*(3), 408-414.

Bansode, A. S., More, S. E., Siddiqui, E. A., Satpute, S., Ahmad, A., Bhoraskar, S. V., & Mathe, V. L. (2017). Effective degradation of organic water pollutants by atmospheric non-thermal plasma torch and analysis of degradation process. *Chemosphere*, *167*, 396-405.

Bogaerts, A., Neyts, E., Gijbels, R., & Van der Mullen, J. (2002). Gas discharge plasmas and their applications. *Spectrochimica Acta Part B: Atomic Spectroscopy*, *57*(4), 609-658.

Braithwaite, N. S. J. (2000). Introduction to gas discharges. *Plasma Sources Science and Technology,* *9*(4), 517.

Capocelli, M., Joyce, E., Lancia, A., Mason, T. J., Musmarra, D., & Prisciandaro, M. (2012). Sonochemical degradation of estradiols: incidence of ultrasonic frequency. *Chemical Engineering Journal*, *210*, 9-17.

De Moraes, S. G., Freire, R. S., & Duran, N. (2000). Degradation and toxicity reduction of textile effluent by combined photocatalytic and ozonation processes. *Chemosphere*, *40*(4), 369-373.

Glaze, W. H., Kang, J.-W., & Chapin, D. H. (1987). The chemistry of water treatment processes involving ozone, hydrogen peroxide and ultraviolet radiation. *Ozone: Science and Engineering*, *9*, 335-352.

Hemmert, D., Shiraki, K., Yokoyama, T., Katsuki, S., Bluhm, H., & Akiyama, H. (2003). *Optical diagnostics of shock waves generated by a pulsed streamer discharge in water.* Paper presented at the Digest of Technical Papers. PPC-2003. 14th IEEE International Pulsed Power Conference (IEEE Cat. No. 03CH37472).

Huang, F., Chen, L., Wang, H., Feng, T., & Yan, Z. (2012). Degradation of methyl orange by atmospheric DBD plasma: Analysis of the degradation effects and degradation path. *Journal of Electrostatics*, *70*(1), 43-47.

Jiang, B., Zheng, J., Qiu, S., Wu, M., Zhang, Q., Yan, Z., & Xue, Q. (2014). Review on electrical discharge plasma technology for wastewater remediation. *Chemical Engineering Journal*, *236*, 348-368.

Kogelschatz, U. (2003). Dielectric-barrier discharges: their history, discharge physics, and industrial applications. *Plasma Chemistry Plasma Processing*, *23*(1), 1-46.

Kuraica, M., Obradović, B., Manojlović, D., Ostojić, D., & Purić. (2006). Application of coaxial dielectric barrier discharge for potable and waste water treatment. *Ind. Eng. Chem. Res.*, *45*, 882-905.

Li, H., Fei, G. T., Fang, M., Cui, P., Guo, X., Yan, P., & De Zhang, L. (2011). Synthesis of urchin-like Co₃O₄ hierarchical micro/nanostructures and their photocatalytic activity. *Applied Surface Science*, *257*(15), 6527-6530.

Li, X., Wang, L., & Wang, B. (2017). Optimization of encapsulation efficiency and average particle size of Hohenbuehelia serotina polysaccharides nanoemulsions using response surface methodology. *Food Chemistry*, *229*, 479-486.

Locke, B., Sato, M., Sunka, P., Hoffmann, M., & Chang, J.-S. (2006). Electrohydraulic discharge and nonthermal plasma for water treatment. *Industrial Engineering Chemistry Research*, *45*(3), 882-905.

Myers, R. H., Montgomery, D. C., & Anderson-Cook, C. M. (2016). *Response surface methodology: process*

and product optimization using designed experiments. New York: John Wiley & Sons.

Quanhong, L., & Caili, F. (2005). Application of response surface methodology for extraction optimization of germinant pumpkin seeds protein. *Food Chemistry*, *92*(4), 701-706.

Qutub, N., Pirzada, B. M., Umar, K., & Sabir, S. (2016). Synthesis of CdS nanoparticles using different sulfide ion precursors: formation mechanism and photocatalytic degradation of Acid Blue-29. *Journal of Environmental Chemical Engineering*, *4*(1), 808-817.

Reddy, P. M. K., Raju, B. R., Karuppiah, J., Reddy, E. L., & Subrahmanyam, C. (2013). Degradation and mineralization of methylene blue by dielectric barrier discharge non-thermal plasma reactor. *Chemical Engineering Journal*, *217*, 41-47.

Schriver, D., Ashour-Abdalla, M., & Richard, R. L. (1998). On the origin of the ion-electron temperature difference in the plasma sheet. *Journal of*

Geophysical Research: Space Physics, *103*(A7), 14879-14895.

Wang, H., Guo, H., Wu, Q., Zhou, G., & Yi, C. (2016). Effect of activated carbon addition on H_2O_2 formation and dye decoloration in a pulsed discharge plasma system. *Vacuum*, *128*, 99-105.

Wang, L., Yu, Z., Peng, Z., Chen, Y., Xiang, G., Liu, Q., . . . Chen, D. (2016). Catalytic properties of TiO_2/Fe_3O_4 nanoparticles in plasma chemical treatment. *Russian Journal of Physical Chemistry A*, *90*(4), 777-782.

Wardenier, N. (2016). *Non-equilibrium plasma in contact with water as advanced oxidation process for decomposition of micro pollutants*. (Master thesis). Gent University.

Xiang, Q., Yu, J., & Wong, P. K. (2011). Quantitative characterization of hydroxyl radicals produced by various photocatalysts. *Journal of Colloid Interface Science*, *357*(1), 163-167.